

Plasmon dispersion in dilute 2D electron systems: Quantum-Classical and Wigner Crystal-Electron Liquid Crossover

E. H. Hwang and S. Das Sarma

Department of Physics, University of Maryland, College Park, Maryland 20742-4111

(October 30, 2018)

We theoretically calculate the finite wave vector plasmon dispersion in a low density 2D electron layer taking into account finite temperature, finite layer width, and local field corrections. We compare our theoretical results with recent Raman scattering spectroscopic experimental 2D plasmon dispersion data in GaAs quantum wells at very low carrier densities ($r_s > 10$) and large wave vectors ($q \geq k_F$). We find good agreement with the experimental data, providing an explanation for why the experimentally measured dispersion seems to obey the simple classical long wavelength 2D plasmon dispersion formula. We also provide a critical discussion on the observable manifestations of the quantum-classical *and* the Wigner crystal - electron liquid crossover behavior in the 2D plasmon properties as a function of electron density and temperature in GaAs quantum well systems.

PACS Number : 73.20.Mf, 73.21.-b, 71.45.Gm

A plasmon (or, a plasma excitation) is a fundamental elementary excitation of an electron system (or, for that matter, any charged particle system). It is the collective (normal) mode of charge density oscillation in the free carrier system, which is present both in classical and quantum plasmas. Studying the collective plasmon excitation in the electron gas has been among the very first theoretical quantum mechanical many body problems studied in solid state physics dating back to the early 1950s¹⁻³. A great deal of theoretical and experimental work has been carried out during the last fifty years on the issue of observable many body effects in the plasmon dispersion relation, originally in the context of bulk metals⁴ and more recently for two dimensional (2D) plasmons⁵ occurring in 2D electron gases confined in semiconductor inversion layers, heterojunctions, quantum wells, and superlattices. The specific theoretical issue is that the plasmon frequency (ω_p) is exactly known only at long wavelengths ($q \rightarrow 0$) where the f -sum rule fixes the plasma frequency to be necessarily that given by classical electrodynamics, namely, $\omega_p = (2\pi n e^2/m)^{1/2} \sqrt{q}$ in 2D and $\omega_p = (4\pi n e^2/m)^{1/2}$ in 3D where n is the 2D (3D) electron density and e^2 is interpreted as $e^2 \rightarrow e^2/\kappa$ where κ is the background lattice dielectric constant. At finite q , away from the long wavelength limit, there are several corrections to the plasmon dispersion $\omega_p(q)$ arising from nonlocal (finite wave vector) response, finite temperature thermal corrections, many-body effects, local field corrections, and other mechanisms relevant to the specific electron system being studied (e.g., finite width of the 2D layer, band structure effects, interface effects, mode coupling effects to phonon and other possible elementary excitations, impurity scattering or disorder effects, etc.). Significant deviations from the long wavelength classical result are predicted to occur⁵⁻¹⁰ in 2D (as well as in 3D⁴ — in this paper we restrict our considerations, motivated by recent experiments¹¹, entirely to 2D plasmons) plasmon dispersion as the electron density is lowered, and the plasmon

wave vector ceases to be in the long wavelength limit ($q \ll k_F$, where $k_F = (4\pi n/g)^{1/2}$, with g as the degeneracy factor of the 2D electron system including spin, is the 2D Fermi wave vector) and starts becoming comparable ($q \approx k_F$) to the Fermi wave vector. Using the usual dimensionless electron gas (quantum) coupling strength parameter r_s ($\equiv 1/a_B \sqrt{\pi n}$, where a_B ($\equiv \hbar^2/m e^2$) is the effective Bohr radius), where r_s is the ratio of the noninteracting kinetic energy to the average potential energy at $T = 0$, one expects large finite wave vector corrections to the classical long wavelength plasmon dispersion relation $\omega_{cl}(q) = \omega_0 \sqrt{q}$, with $\omega_0^2 = 2\pi n e^2/m$, for $r_s \gg 1$ where the electron gas is strongly interacting. In fact, there are theoretical predictions, based on model many-body plasmon dispersion calculations¹⁰, that the 2D plasmon frequency may renormalize to zero at finite wave vectors (and $r_s \gg 1$) due to interaction-induced softening of the plasmon dispersion. In general, theories including higher order many-body and other effects predict a lowering of the plasma frequency below the classical plasmon dispersion curve for $r_s > 1$ and finite values of q/k_F .

It therefore comes as a surprise that recent inelastic light (Raman) scattering based direct measurements¹¹ of 2D plasmon dispersion in high quality low density (down to electron densities as low as $n \approx 5 \times 10^8 \text{ cm}^{-2}$ corresponding to r_s parameter as high as 25) electron systems in GaAs quantum wells find remarkably good agreement between the measured 2D plasmon dispersion and the simple classical formula ($\omega_p \approx \omega_{cl}$) upto wave vectors as large as $q \sim 2k_F$. Earlier experimental measurements¹² of 2D plasmon dispersion in semiconductor structures were typically restricted to higher carrier densities ($r_s \leq 1$) and lower wave vectors ($q \sim 0.1 - 0.2k_F$) where the classical $q^{1/2}$ plasmon dispersion relation is valid by virtue of the applicability of the long wavelength f -sum rule. A primary motivation for the recent low electron density 2D plasmon dispersion measurement¹¹, which we are trying to theoretically un-

derstand in this paper, has been to explore high-wave vector ($q \geq k_F$) and low density ($r_s \gg 1$) dispersion corrections to the classical $q^{1/2}$ 2D plasmon dispersion formula. The unexpected finding¹¹ that the experimental 2D plasmon dispersion follows quantitatively the classical $q^{1/2}$ formula upto large values of q/k_F (~ 2) even for very strongly interacting ($r_s \sim 25$) 2D electron systems is a significant puzzle, particularly in view of the extensive existing theoretical literature⁵⁻¹⁰ on finite wave vector many-body and nonlocal plasmon dispersion corrections showing very large deviations from the classical plasma frequency.

By carrying out a realistic random phase approximation (RPA) calculation of the finite temperature, finite wave vector 2D plasmon dispersion in the actual GaAs quantum wells used in ref. 11, we provide a partial resolution of the puzzle posed by the data presented in ref. 11. In particular, we show that RPA provides an excellent quantitative description of the data — the nonlocal finite q corrections introduced by RPA (which are substantial for $q/k_F \sim 2$) are not explicitly manifest in the experimentally measured plasmon dispersion¹¹ because of a fortuitous cancellation among a number of independent contributions to the plasmon energy, mostly the almost exact accidental numerical calculation between the higher-order (i.e., $q^{3/2}$ and higher) nonlocal finite wave vector correction (tending to increase the plasma frequency above the classical dispersion curve and becoming quantitatively prominent for $q/k_F > 1$) and the finite layer width correction arising from the *quasi*-2D nature of the electron layer (which by itself lowers the plasma frequency below the classical dispersion curve because the usual q^{-1} Coulomb interaction in a strictly 2D system is softened in the *quasi*-2D system, and this softening induced lowering of the plasma frequency is particularly quantitatively significant in low density systems, where the layer width in the transverse direction is large due to the weakening of the Hartree selfconsistent potential contribution to the confinement). We also find, as explained below, that a slight ($\sim 10\%$) adjustment in the quoted sample densities in ref. 11, where density has not been independently measured but inferred from the measured plasmon dispersion, significantly improves the agreement between our theoretical results and experimental data.

The plasmon dispersion can be calculated by finding poles of the density-density correlation function. Within RPA (or its simple generalizations^{7,9,10} including local field corrections arising from correlation effects) plasmon modes at finite wave vectors and finite temperatures are given by the zeros of the dielectric function, $\epsilon(q, \omega; T) = 1 - v(q)\Pi_0(q, \omega; T)$, where $v(q)$ is the Coulomb interaction modified by both the quasi-2D form factor due to the finite width of the 2D quantum well and correlation-induced local field effects, and $\Pi_0(q, \omega, T)$ is the noninteracting 2D finite temperature irreducible polarizability. The modification of the Coulomb interaction due to correlation induced local field correction is modeled by a static correlation factor $G(q)$, which we calculate within

the Hubbard approximation^{4,7,10}. In the presence of local field corrections the Coulomb interaction is modified in the following manner: $v(q) \rightarrow v(q)[1 - G(q)]$. Note that local field corrections, $0 < G(q) < 1$, tend to soften the Coulomb interaction because exchange-correlation effects tend to keep the electrons away from each other reducing the effective Coulomb interaction. We calculate numerically the plasmon dispersion by solving $\epsilon(q, \omega; T) = 0$ to obtain $\omega_p(q; n, T)$ by incorporating thermal, finite thickness, and local field correlation effects. (All other effects, e.g. phonons, give negligible corrections to the plasmon dispersion in a low density GaAs quantum well electron system.) For each density the chemical potential of the 2D system has to be calculated self-consistently at temperature T since at the low densities of interest to us, where $E_F \sim k_B T$, the chemical potential is very different from the Fermi energy. In our calculation we incorporate finite thickness corrections by using a quasi-2D form factor appropriate for an infinite square well potential with a width d . At the low electron densities used in ref. 11 the infinite square well confinement model is a very good approximation since the Hartree selfconsistent effects are weak. We include the local-field correction^{7,10} using the Hubbard approximation (HA), where the 2D HA correlation factor is given by

$$G(q) = \frac{1}{g} \frac{q}{\sqrt{q^2 + k_0^2}},$$

where $k_0 = k_F$ at $T = 0$. We generalize the $T = 0$ HA^{7,10} to finite temperatures by simply redefining k_0 to be the finite temperature analogy of the Fermi wave vector using the formula: $k_0(T) = k_F(T/T_F) \ln(1 + e^{\mu/k_B T})$, where $\mu = \mu(T) = k_B T \ln[e^{(n/k_B T)(2\pi/gm)} - 1]$ is the finite temperature 2D chemical potential obtained from the total number of particles $n = \int dE D(E)f(E)$, using the 2D electron density of states, $D(E)$, and the Fermi distribution function, $f(E)$. The use of this particular (i.e., HA) local field correction is an uncontrolled approximation of our theory since there is no generally accepted theoretical framework to incorporate correlation effects (beyond RPA) in the plasmon dispersion calculation. Our finite temperature generation of the HA is, however, quite reasonable since it correctly interpolates between the $T = 0$ 2D HA⁷ with $k_0(T = 0) = k_F$ and the high temperature result, $k_0(T/T_F \rightarrow \infty) = 0$, of vanishing local field correction. We have checked that the use of other static local field corrections (e.g. the finite-T STLS corrections¹³) do not significantly alter our conclusion. It is well-known^{4,7} that the HA for the local field correction, while being static and theoretically uncontrolled, has the great advantage of being simple and reasonably quantitatively accurate compared with other local field correction approximations.

In Fig. 1 we show our calculated plasmon dispersion along with the available experimental data from ref. 11. In Figs. 1(a) and 1(b) respectively plasmon dispersion curves for $r_s = 5.2$ ($n = 1.2 \times 10^{10} \text{cm}^{-2}$) and $r_s = 17.2$

($n = 1.1 \times 10^9 \text{ cm}^{-2}$) are shown at $T = 200 \text{ mK}$. We use in our calculations system parameters corresponding to GaAs-Al_xGa_{1-x}As quantum wells with a well width $d = 330 \text{ \AA}$ as appropriate for ref. 11. Thin solid lines represent the classical long wavelength plasmon dispersion ($\omega_{cl} = \omega_0 \sqrt{q}$). Dotted lines show the dispersion including finite wave vector non-local (i.e., higher order in q) effects calculated within RPA, which leads to an increase in plasma frequency compared with ω_{cl} . The leading order RPA dispersion correction is given by $\omega_p(q)/\omega_{cl} = 1 + (3/4)(q/q_{TF})$, where $q_{TF} (= gme^2/\hbar^2)$ is the 2D screening wave vector. Dashed lines are the dispersions including corrections by both non-local and finite thickness effects. Finite well width reduces the plasma frequency by softening the 2D Coulomb interaction, and its long wavelength dispersion in an infinite square well potential model can be calculated by straightforward algebra to be given by $\omega_p(q)/\omega_{cl} = 1 - 0.207(d/a_B)(q/q_{TF})$. Noting that $g = 2$ (spin degeneracy) in GaAs quantum wells, i.e. $q_{TF}a_B = 2$, we find that the two dispersion corrections (non-local and finite width) approximately cancel each other when $3q/4q_{TF} = 0.207dq/a_Bq_{TF}$. Thus we find that non-local effects and finite thickness corrections cancel each other almost exactly in a quantum well with well thickness $d \approx 3.6a_B$. The GaAs ($a_B \approx 90 \text{ \AA}$) sample used in ref. 11 has a quantum well width $d = 330 \text{ \AA}$, which gives rise to an almost exact cancellation between non-local effects and finite thickness corrections. As shown in Fig. 1 RPA results with realistic finite thickness effects agree with the classical formula upto a large wave vector ($q \sim 2k_F$) and provide reasonable quantitative agreement with experimental 2D plasmon dispersion data. Dot-dashed lines in Fig. 1 are the plasmon dispersion curves including local field corrections, non-local dispersion, and finite thickness effects at $T = 0$. The local field corrections tend to reduce the plasma frequency since it softens the Coulomb interaction by keeping the electrons effectively away from each other, and in the long wavelength limit the 2D plasmon dispersion within the HA local field corrections is given at $T = 0$ by $\omega_p(q)/\omega_{cl} = 1 - (r_s/2\sqrt{2})(q/q_{TF})$. As the density decreases (or r_s increases) the reduction of the plasma frequency due to local field corrections is stronger, and this effect dominates in large wave vectors. Thick solid lines show the full plasmon dispersion including finite temperature effects at $T = 200 \text{ mK}$ including all the corrections described above. (Long dashed line represents the plasmon dispersion including all corrections at $T = 200 \text{ mK}$ with zero temperature HA, i.e., $k_0 = k_F$.) Even within RPA finite temperature effect by itself increases the plasma frequency. The thermal enhancement is negligible (exponentially small for $T/T_F \ll 1$) at low T in high density GaAs 2D electron systems since the Fermi temperature in these systems is much greater than the experimental temperature ($T/T_F \ll 1$). However, a very low density electron system (e.g., electrons on the surface of liquid Helium, where the Fermi temperature is

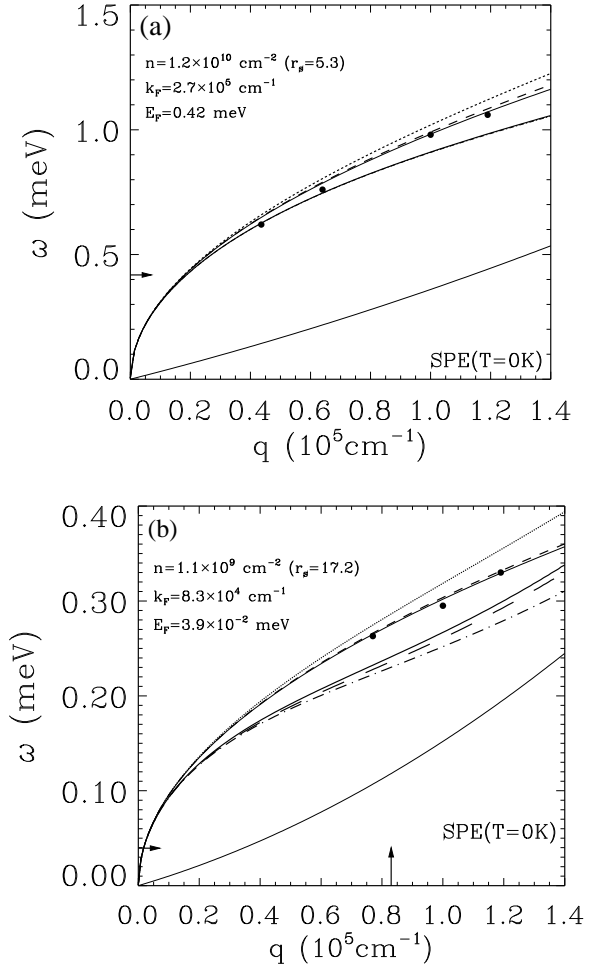


FIG. 1. Calculated plasmon dispersions with available experimental data [11] for (a) $n = 1.2 \times 10^{10} \text{ cm}^{-2}$ ($r_s = 5.3$) and (b) $n = 1.1 \times 10^9 \text{ cm}^{-2}$ ($r_s = 17.2$). Thin solid line is the classical local plasmon dispersion and thick solid line indicates the dispersions with all corrections (as explained in the text) at a finite temperature ($T = 200 \text{ mK}$). Other lines in the figure are described in the text. The arrows indicate the Fermi wave vector and Fermi energy. The dots are experimental data points from ref. [11].

smaller than or comparable with experimental temperature) is essentially a non-degenerate classical plasma, where the long wavelength plasmon dispersion is given by $\omega_p(q)/\omega_{cl} = 1 + (3/2\sqrt{2})(T/T_F)(q/r_s)$. In a quantum plasma ($T \ll T_F$) on the other hand the leading order thermal correction to the $T = 0$ plasmon dispersion is exponentially weak in temperature. We thus see that for T/T_F not too small (which is the experimental situation in ref. 11, where $T/T_F \approx 0.4$ at the lowest density) the thermal correction to the plasma frequency tends to cancel the local field correction similar to the cancellation between the nonlocal finite q corrections and quasi-2D finite width corrections.

In Fig. 1(a) the plasmon dispersion for $r_s = 5.3$ ($n = 1.2 \times 10^{10} \text{ cm}^{-2}$) is shown. In this relatively high

density system the experimental data lie in the long wavelength ($q < k_F = 2.7 \times 10^5 \text{cm}^{-1}$) and the low temperature ($T \ll T_F = 5.0\text{K}$) limit. Note that the enhancement of plasma frequency by non-local effects is almost cancelled by finite thickness effects. The local field corrections and finite temperature effects are not important in this sample since these effects are quantitatively significant only at low n or large r_s . In Fig. 1(b) we show the plasmon dispersion for $r_s = 17.2$ ($n = 1.1 \times 10^9 \text{cm}^{-2}$). Experiment data¹¹ for this sample lie in the effective large wave vector ($q > k_F = 0.83 \times 10^5 \text{cm}^{-1}$) regime. Even in this low density sample (and at large effective wave vectors) the experimental data can be seen to agree very well with the classical plasma dispersion and the finite thickness RPA calculations. Since the non-local effects are almost canceled by the finite width correction, we speculate that the reduction of the plasma frequency due to local field corrections is perhaps almost exactly canceled by the thermal enhancement of the plasma frequency. Our calculated results (Fig. 1(b)), however, show the local field corrections to be too large in this low density sample to cancel out with thermal effects. It is certainly possible, perhaps even likely, that our calculated HA local field corrections are strong overestimations of the actual finite temperature ($T/T_F \sim 0.4$ in the experiment) local field corrections, and in reality local field corrections, being much smaller than our HA results, do in fact cancel out with the finite temperature enhancement. This remains an important open question for future theoretical work. One would need a quantitatively more accurate and theoretically well-controlled finite temperature theory for local field corrections for this purpose. At present no such local field theory exists in the theoretical literature.

Since the local field corrections (even within HA) are regarded as improvement to RPA in calculating many physical properties of low density systems (strongly correlated systems) the large discrepancy between the plasmon mode dispersion (in Fig. 1(b)) including local field effects and the experimental data in this low density electron system is unexpected. It is troublesome to uncritically accept that correlation effects are negligible based on the mere speculation that finite temperature local field corrections may be small (in other words, much smaller than what we calculate within the HA). We now suggest another possibility. In ref. 11 the electron densities are estimated using the classical local plasmon dispersion formula based on the fact that the \sqrt{q} dispersion seems to apply very well to the experimental plasma dispersion. This could, however, be problematic, and may in fact lead to an underestimation of n . We now compare the zero temperature classical local plasmon formula used to estimate the electron densities given in ref. 11 ($n = 1.1$ and $3.7 \times 10^9 \text{cm}^{-2}$) with the corresponding finite temperature plasmon dispersion including all the corrections described above, using somewhat higher densities in the complete dispersion calculation. In Fig. 2 we show the plasmon dispersion including all corrections for densities

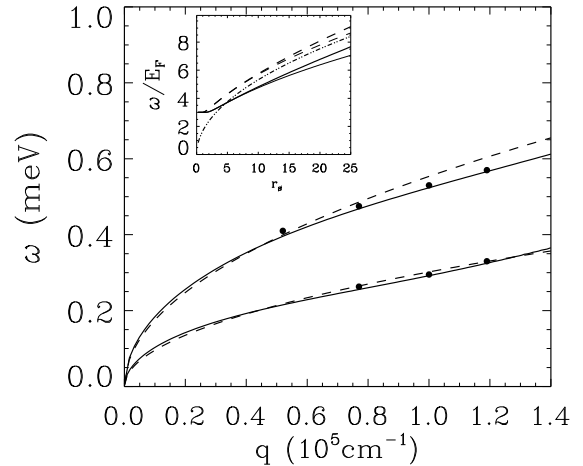


FIG. 2. Comparison of finite temperature ($T = 200\text{mK}$) plasmon dispersions (solid lines) including all corrections for the density $n = 1.37, 4.1 \times 10^9 \text{cm}^{-2}$ with zero temperature classical local dispersions (dashed lines) for $n = 1.1, 3.7 \times 10^9 \text{cm}^{-2}$. Experimental data are taken from ref. [11]. Inset shows the plasma frequency as a function of density parameter r_s at $q = k_F$. Dot dashed line is the classical plasmon mode, dashed lines are RPA modes (thick line for $T = 300\text{mK}$ and thin line for $T = 0\text{K}$), and solid lines are HA modes (thick line for $T = 300\text{mK}$ and thin line for $T = 0\text{K}$).

$n = 1.37$ (lower solid line) and $4.1 \times 10^9 \text{cm}^{-2}$ (upper solid line). Experimental data points are taken from ref. 11. Dashed lines in Fig.2 are the classical $T = 0$ local plasmon dispersion for the density $n = 1.1$ (lower line) and $3.7 \times 10^9 \text{cm}^{-2}$ (upper line). Our calculated full plasmon dispersion in Fig. 2 for somewhat higher densities including all corrections also agrees very well with experiment just as the classical $T = 0$ formula apparently does for the lower densities proposed in the experiment. Thus, whether the local field corrections are large or not is not obviously clear until one can measure the experimental electron density using an independent method. This is, however, very difficult to do in the interesting regime of very low electron densities where the usual Hall density measurement fails. At this stage all we can say is that the full plasmon dispersion (including local field corrections and the other effects) could explain the experimental data provided one uses somewhat larger electron densities than the experimental carrier density estimates (based on a comparison of the data with the classical $T = 0$ plasma dispersion formula) in ref. 11. Inset in Fig. 2 shows the quantum-classical crossover of the plasma frequency at wave vector $q = k_F$ and $T = 300\text{mK}$ as a function of the density parameter r_s . In the high density limit the enhancement of the plasma frequency by non-local effects dominates all other corrections, but in the low density limit the local field corrections give rise to a large decrease of the plasma frequency. Thermal correction of the plasmon mode also increases as the density decreases.

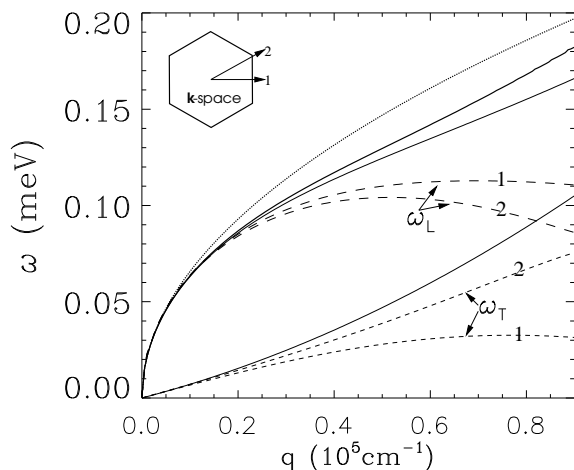


FIG. 3. Comparison of plasmon dispersions calculated within HA (solid lines, the thick and thin line being for $T = 200\text{mK}$ and $T = 0\text{K}$, respectively) with the phonon modes of a hexagonal Wigner lattice (dashed lines) for $r_s = 25$. The dotted line is the classical plasmon dispersion.

In Fig. 3 we compare the plasmon dispersion calculated within the quantum HA with the “phonon” modes of the electron solid (hexagonal Wigner crystal (WC)¹⁴) within the harmonic approximation upto the zone boundary of the lattice for $r_s = 25$ (corresponding to an electron density, $n = 5.4 \times 10^8\text{cm}^{-2}$, for the 2D GaAs system). Inset shows the hexagonal Wigner lattice in the momentum space. ω_L (ω_T) indicates the longitudinal (transverse) phonon mode of the 2D Wigner lattice. The longitudinal WC phonon mode (which corresponds to the plasmon in the electron liquid system) has much lower frequency than the quantum plasmon mode at $r_s = 25$, which is consistent with the fact that the transition to a WC phase is expected to occur at substantially lower electron densities (around $r_s = 37$ or below). In the long wave length limit the WC phonon mode agrees with plasmon mode within HA. But in the high wave vector region $q > k_F$ ($k_F = 5.7 \times 10^4\text{cm}^{-1}$), we find that the HA plasmon mode has a much higher frequency than the optical phonon mode. The experimentally measured plasmon dispersion in ref. 11 is also much higher than the WC results shown in Fig. 3 indicating that the WC physics is unlikely to be playing a role here.

In considering the transition to the low density WC phase (and in particular whether the plasmon, or more appropriately the longitudinal optical phonon, mode in the electron crystal phase could be observed in low density 2D GaAs based electron systems) we show in Fig. 4 our best (approximate) estimate for the 2D electron liquid/crystal phase diagram (appropriate for 2D GaAs based electron systems) in the density-temperature (n, T) plot. The classical WC - electron liquid (first order) phase transition line is defined by $\Gamma = \Gamma_c$, where $\Gamma = \langle V \rangle / \langle T \rangle$, where $\langle V \rangle = e^2(\pi n)^{1/2}$ is the classical mean potential energy and $\langle T \rangle$ is the mean classical kinetic energy given by

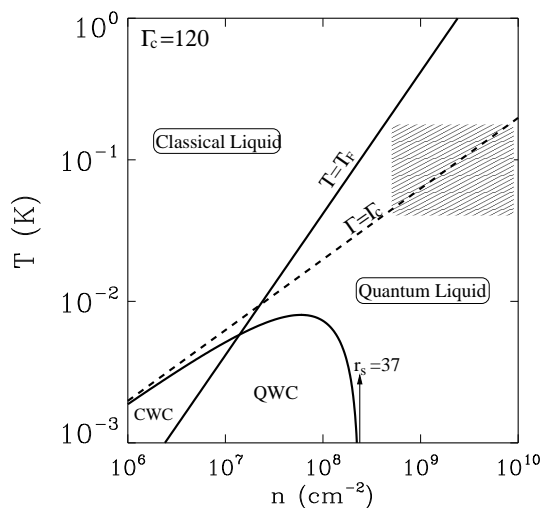


FIG. 4. Calculated 2D electron liquid - Wigner crystal phase diagram in the density - temperature (n, T) plot (appropriate for GaAs systems). The QWC (CWC) represents the quantum (classical) Wigner crystal.

$$\langle T \rangle = \frac{2}{n} \int \frac{d^2p}{(2\pi)^2} \frac{\hbar^2 p^2}{2m} n_F(p),$$

where $n_F(p)$ is the finite temperature Fermi distribution function, and Γ_c is found from numerical (molecular dynamics) simulations¹⁵ to be $\Gamma_c \approx 120$. The high temperature region above the $\Gamma = \Gamma_c$ line (dashed line), $\Gamma < \Gamma_c$, in Fig. 4 is a classical Coulomb liquid (for $T > T_F$) whereas the low T region below the $\Gamma = \Gamma_c$ line, $\Gamma > \Gamma_c$, is the classical Wigner crystal (CWC), for $T > T_F$. At zero (low) temperature quantum fluctuations produce a (first order) quantum phase transition between the (low density) electron crystal phase and the (high density) electron liquid phase. At $T = 0$ this transition occurs at $r_s = r_s^*$ where the critical r_s^* is found¹⁶ by quantum Monte Carlo simulations to be around $r_s^* = 37$. The high density region ($r_s < r_s^*$) in Fig. 4 to the right of the $r_s = r_s^*$ (at $T = 0$) line is the quantum liquid whereas the low density region ($r_s > r_s^*$) along the $T = 0$ line is the quantum Wigner crystal (QWC). We have produced the (n, T) phase diagram in Fig. 4 using a simple mean field theory and Padé approximation, which smoothly interpolates between the classical result $\Gamma = \Gamma_c$ as $n \rightarrow 0$ and the quantum result $r_s = r_s^*$ as $T \rightarrow 0$. The experimental regime explored in ref. 11 is shown as the shaded block in Fig. 4, and we have added the $T = T_F$ line to crudely separate the classical and quantum regimes. From Fig. 4 it is clear that the samples used in ref. 11 are essentially in the quantum electron liquid region — increasing T (both decreasing n and T) one should be able to explore the classical liquid (Wigner crystal) region. We propose that plasmon experiments be carried out in the lowest density samples at higher temperatures ($T \geq 4\text{K}$) in order to test the quantum-classical crossover in the 2D plasmon properties.

Finally in Fig. 5 we show our predicted plasmon

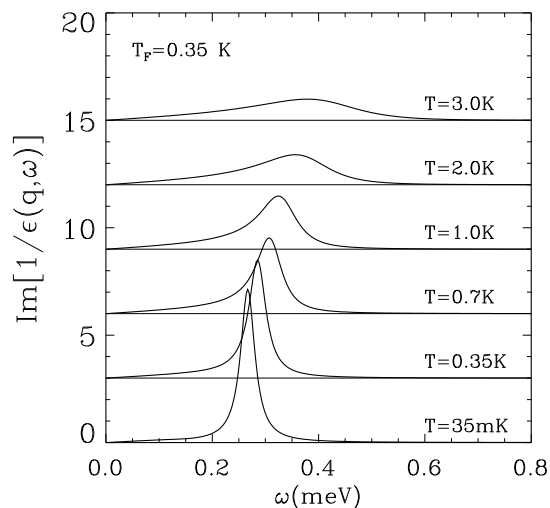


FIG. 5. The plasmon spectral weight (or the loss function, $\text{Im}[1/\epsilon(q, \omega)]$) at a low 2D electron density, $r_s = 18.4$ ($n = 0.85 \times 10^9 \text{cm}^{-2}$) for various temperatures at a given wave vector $q = 10^5 \text{cm}^{-1}$. The Fermi temperature of this system is $T_F = 350 \text{mK}$. We include an impurity level broadening of 0.05meV in this calculation.

behavior in the classical ($T > T_F$) regime, which should be easily achievable (see Fig. 4) in the lowest density samples of ref. 11 simply by raising the temperature to 3 – 4K. One should observe spectacular thermal level broadening of the plasmon peak (as well as a temperature induced high energy blue shift of the plasmon energy) as shown in Fig. 5. This spectacular level broadening will indicate the quantum-classical plasmon crossover — the current data in ref. 11 are all essentially still in the quantum regime. Observation of the WC collective modes will, however, require samples with substantially lower carrier densities (and lower temperature measurements) as indicated in our phase diagram in Fig. 4.

We conclude by summarizing our results: We have obtained reasonable agreement with the measured plasmon dispersion¹¹ in low density 2D systems by carrying out a complete quantitative calculation of 2D plasma dispersion. We find considerable cancellations among various physical mechanisms (e.g., between non-local effects and finite width corrections and between thermal effects and local field corrections) in the plasmon dispersion leading to the observed apparent agreement¹¹ between experiment and classical 2D plasma dispersion formula. We also study the quantum-classical as well as crystal-liquid crossovers in the 2D plasmon behavior and propose specific experimental studies to test our theoretical predictions.

This work is supported by the U.S.-ONR.

- ¹ S. Tomonaga, Prog. Theor. Phys. (Kyoto) **5**, 544 (1950).
- ² D. Bohm and D. Pines, Phys. Rev. **82**, 625 (1951); **85**, 332 (1953); **92**, 609 (1955).
- ³ J. Lindhard, Kgl. Dan. Vidensk. Selsk. Mat. Fys. Medd. **28**, 8 (1954).
- ⁴ D. Pines and P. Nozières, *The Theory of Quantum Liquids* (Addison-wesley, New York, 1989); G. D. Mahan, *Many-Particle Physics* (Plenum, New York, 1990); N. H. March, *Electron Correlations in Molecules and Condensed Phases* (Penum, New York, 1996).
- ⁵ T. Ando, A. B. Fowler, and F. Stern, Rev. Mod. Phys. **54**, 437 (1982); references therein.
- ⁶ D. E. Beck and P. Kumar, Phys. Rev. B **13**, 2859 (1976); **14**, 5127 (1976); A. K. Rajagopal, Phys. Rev. B **15**, 4264 (1977).
- ⁷ M. Jonson, J. Phys. C **9**, 3055 (1976); N. Iwamoto, Phys. Rev. B **43**, 2174 (1991).
- ⁸ P. M. Platzman and N. Tzoar, Phys. Rev. B **13**, 3197 (1976); N. Studart and O. Hipólito, Phys. Rev. B **22**, 2860 (1980).
- ⁹ A. Czachor, A. Holas, S. R. Sharma, and K. S. Singwi, Phys. Rev. B **25**, 2144 (1982); A. Holas and K. S. Singwi, Phys. Rev. B **40**, 158 (1989).
- ¹⁰ D. Neilson *et al.*, Phys. Rev. Lett. **71**, 4035 (1993); Phys. Rev. B **44**, 6291 (1991); S. Das Sarma and E. H. Hwang, Phys. Rev. Lett. **81**, 4216 (1998).
- ¹¹ M. A. Eriksson *et al.*, Physica E **6**, 165 (2000); A. Pinczuk *et al.*, unpublished.
- ¹² S. J. Allen, Jr., D. C. Tsui, and R. A. Logan, Phys. Rev. Lett. **38**, 980 (1977); T. N. Theis, J. P. Kottaus, and P. J. Stiles, Solid State Commun. **24**, 273 (1977); T. N. Theis, Surf. Sci. **98**, 515 (1980).
- ¹³ L. Liu *et al.*, Physica B **249-251**, 937 (1998).
- ¹⁴ R. S. Crandall, Phys. Rev. A **8**, 2136 (1973); L. Bonsall and A. A. Maradudin, Phys. Rev. B **15**, 1959 (1977).
- ¹⁵ R. C. Gann, S. Chakravarty, and G. V. Chester, Phys. Rev. B **20**, 326 (1979); M. Imada and M. Takahashi, J. Phys. Soc. Jpn. **53**, 3770 (1984).
- ¹⁶ B. Tanatar and D. M. Ceperley, Phys. Rev. **39**, 5005 (1989).